Aalborg University

Materials Technology

Prediction of the Hardness in the HAZ of S890QL as a Function of Cooling Time

Author
Nina Samodajev

Supervisor
Mikael Larsen
Jens. H.Andreasen

June 29, 2018

AALBORG UNIVERSITY
STUDENT REPORT

Department of Mechanical and Manufacturing Engineering
Fibigerstræde 16 DK - 9220 Aalborg East
Phone +45 99 40 71 10
lft@m-tech.aau.dk

Title:
The Prediction of the Hardness in the HAZ of S89QL as a Function of Cooling Time

Semester:
Master thesis

Semester theme:
Master thesis in Welding Metallurgy

Project period: 01.03 - 29.06.2018

ECTS:
30

Supervisor: Mikael Larsen
Jens C Andreasen

Nina Samodajev

Number printed: []
Pages: [41]
Pages Appendix: []
Enclosures: [29.06.2108]

ABSTRACT:

This master thesis investigated the effect of welding parameters, such as welding heat input, preheat temperature and cooling time on the hardness of the HAZ of high strength steel, S890QL. Different approaches have been used in order to determine the micro-structural changes and hardness in the HAZ as a function of cooling time. First, analytical heat flow Rosenthal's approach was used to calculate the temperature distribution and to introduce the effect of cooling time on the micro-structural changes. Second, the hardness the along the Jominy sample as a function of cooling time was measured and compared to Terasaki's predicted hardness method. The 3D Simulation of Rosenthal modelling have gave showed that cooling time increases when het input and preheat temperatures increases. Cooling time controls the micro-structural changes and defines the hardness of the material. The predicted and measured hardness showed a good agreement. Therefore, an estimation of the maximum HAZ hardness can be predict from these models and this approach can substantially reduce the number of welding qualifications test.

By signing this document, each member of the group confirms participation on equal terms in the process of writing the project. Thus, each member of the group is responsible for the all contents in the project.

Preface

This master's thesis was written as a last step towards a two-year master's degree in Materials Technology at Aalborg University. Work was initiated in March 2018 and finished in June the same year, under the supervision of Mikael Larsen and Jens. H.Andreasen. The project was made in collaboration with Liftra who also provided the feedstock material for the project.

First, the gratitude to the lab technicians in the workshop of the Department of Materials and Production, for the huge help in preparing the necessary equipment and material for the project. Next, I would thanks to my supervisors, Mikael Larsen and Jens. H.Andreasen for their interest in advising me and thus making this possible. A really special thanks to my family and friends who gave me all the support to make this this happen. One more special thanks is going to Amanda Salazar del Campo for her astounding support and help with data design.

Contents

1 Introduction **1**
- 1.1 Initial investigation based on the previous project 2
- 1.2 Additional hardness analyses of HAZ 5
- 1.3 Aim of the project 8

2 Heat flow theory **9**
- 2.1 Heat flow 9
- 2.2 Rosenthal's equations 11

3 Hardenability of steel **19**
- 3.1 Transformations during cooling 20

4 Hardness prediction model **23**
- 4.1 Terasaki model 24

5 Method, results and discussion **27**
- 5.1 Methodology 27
  - 5.1.1 Experimental set-up 27
  - 5.1.2 Procedure 27
- 5.2 Results and discussion 30
  - 5.2.1 Rosenthal modelling 30
  - 5.2.2 Jominy simulations 31
  - 5.2.3 The predicted and measured hardness curves 39

6 Conclusion of the investigations **40**

References **41**

Chapter 1

Introduction

The present scale of modern, welded construction is quite remarkable. The wide range of materials used to build extremely large constructions should fulfill requirements of high strength, good toughness, and hardness. Moreover, it is essential that the materials possesses good weldability, [10]. As the weld zone is one of the weakest point of a structure, it is essential that material posses good weldability. On that premise, heat control and tougher filler metals represent a challenge for the welding operators as, in high strength steels, this will determine the behaviour of the material, [9]. Therefore, the first step toward a successful welding is to understand a type of welding process, materials composition and mechanical properties of high strength steels.

The influence of preheating high strength steel(HSS) S890QL butt welded joint and its mechanical behaviour has been the focus of the investigation through the 9th-semester project at Aalborg University. The main focus was to investigate differences in mechanical properties of not-preheated and preheated samples. Results from toughness and hardness measurements showed that small differences were obtained between the tested samples. From a manufacturing point of view, those conclusions can help in choosing a welding process which will provide savings in time and costs of welding a HSS.

However, it was noticed during hardness testing that hardness values in heat affected zone (HAZ) showed lower values than in the rest of material, which was observed in both, not-preheated and preheated samples. Since the amount of the samples that were subjected to hardness measurements in the previous project was very low, new hardness measurements are performed and a better understanding of the influence of the welding parameters, such as heat input and preheat treatments on the weld joint of a HSS is discussed. Furthermore, it was found that the lower hardness values could be related to the performance of a welding procedure. The micro-structure of a HAZ is changed during welding due to influence of thermal cycles and cooling process in between. To achieve minimal changes in the HAZ, it is necessary to consider how the micro-structure of the base metal reacts to the complete thermal cycle, i.e. the heating cycle, the peak temperature and finally, the cooling cycle and its effect on the phase transformations in the material, [9].

Therefore, the problem is to determine the influence of the welding parameters, i.e. preheat input, cooling time and welding speed, on the mechanical properties; toughness,

strength, and hardness of a high strength steel, S890QL. In the last semester, physical behaviour of the material has been measured by different experiments. Impact toughness values showed significant results for the samples which were subjected to different preheat treatments. Hardness values in HAZ showed slightly drop in comparison to weld and base material. However, other studies also showed that metallurgical and weldability issues related to the HAZ characteristics are quite difficult to understand, [15], [19]. In general, different regions of HAZ of high strength steels have been defined and characterized by performing a weld thermal simulations on the base material using a specific peak temperature, [9]. These simulations of weld thermal cycles under laboratory conditions are used in order to obtain information about micro structural and property changes in the HAZ, [9]. The steel in the HAZ undergoes rapid heating from the welding arc followed by a cooling process, [11], [10]. It is important to understand how cooling time is associated to a given heat input, steel thickness, weld geometry, etc.
To characterise the effect of thermal cycles, Rosenthal heat-flow theory will be used in order to examine temperature distribution within the sample. Next, the Jominy end-quenched test will be used to predict the hardness as a function of the cooling curves. Lastly, estimated cooling curves in combination with time-temperature diagrams should help in the prediction of hardness as a function of a cooling time.
The following section contains an initial investigation based on the results from the previous project, with focus on the influence of the welding process on the mechanical properties of HAZ.

1.1 Initial investigation based on the previous project

In general, high strength steels should be preheated to some temperatures before welding. Preheating minimizes the temperature difference between the welding arc and the base material, slows the rate of cooling in the finished weld and it helps to reduce shrinkage stresses that can lead to cracking,[18], [9]. While slowing the cooling rate it helps to reduce the hardness in the HAZ, [9]. However, results from the 9th-semester project showed that tensile strength, hardness and impact toughness of the high strength steel S890QL which was not exposed to a preheating treatment, provided the same result as in not-preheated samples.
When producing or fabricating materials in order to meet service requirements, materials and metallurgical engineers must have an understanding of the relationships between the micro-structure of materials and their mechanical properties. Therefore, in order to understand how the influence of preheating the HSS S890QL has affected the welded joints, certain mechanical testings have been performed. This section will provide a brief overview of mechanical results from the previous project in order to provide a better understanding of the effects which will be further investigated.

Impact Toughness

The brittle fractures for welded structures often occur at relatively low ambient temperatures, however, the impact toughness values from both, not-preheated and preheated samples exceeded the standard values of -27J for the samples cooled at -40°C, (Fig.1.1). The figure shows 27 measurements for each notch location, for both not-preheated and preheated samples with calculated deviations.

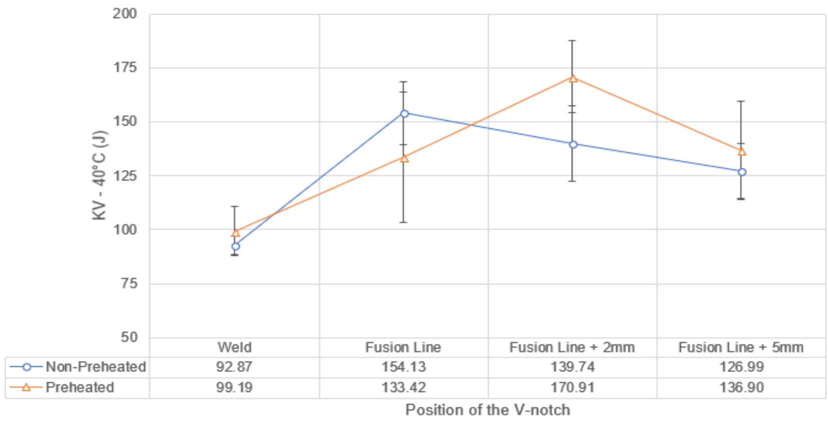

Figure 1.1: Differences in impact toughness values between not-preheated and preheated samples

The toughness in the weld of both not-preheated and preheated samples showed similar values, 92J and 99J, respectively. Away from the weld material, at the fusion line, preheated samples experienced rise in impact values followed by a drop in the region 2mm from the fusion line. However, the not-preheated samples showed the loss of ductility in the region where preheated samples experineced the rise.
This phenomena was also experienced in research of Akselsen et.al. [19]. They investigated HAZ strength and ductility as a function of cooling time between three different high strength steels. They found that ductility is generally reduced at fast cooling rates ($\Delta t_{8-5} < 8s$) because of the formation of brittle martensite phases.
However, it was expected that preheating will give more time for HAZ zone to cool down and form micro-structure which is higher in toughness. Although, the ductility of HAZ of not-preheated samples was reduced in comparison to preheated samples, the obtained values are more than acceptable according to standards,[1].

Tensile strength

Determination of material's strength was performed by standard tensile tests, according to EN ISO 6892-1, [2].

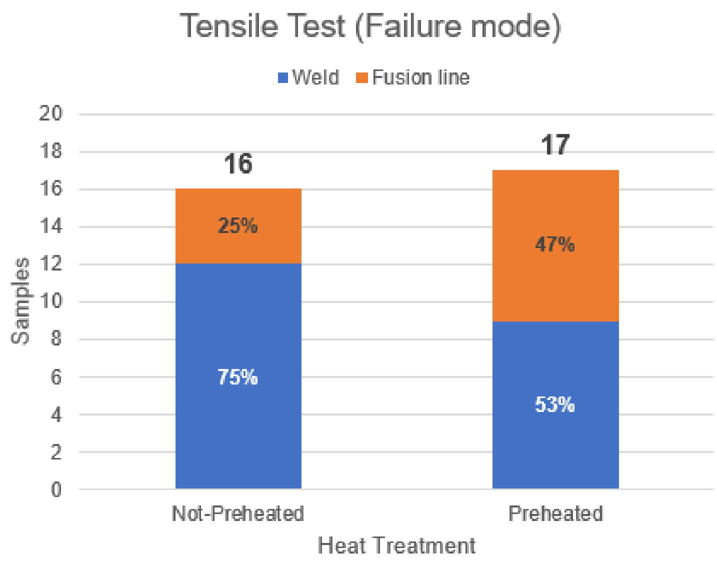

Figure 1.2: Measured tensile strength and observed tensile failures of the investigated material, S890QL

	Failure	Max. Tensile Value	Average
Not-Preheated	Fusion line	1060	1038.5 ± 14.39
	Weld	1051	1024.3 ± 18.20
	Total	1060	1027.3 ± 18.01
Preheated	Fusion line	1044	1033.5 ± 7.52
	Weld	1060	1039.3 ± 15.99
	Total	1060	1036.4 ± 12.67

Table 1.1: The maximum tensile values and measured deviations

The tensile results in the Fig.1.2 showed that preheated weld joints experienced a higher amount of fracture in the fusion line in comparison to the weld joint that were not preheated. This is proposed to be due to the effect of preheating on the increase of the cooling time which promoted weaker micro-structures in HAZ. The table is representing the maximum value in each of the both case.
Akselsen et.al. ([19], have found that HAZ yield and tensile strength are rapidly reduced with an increase in cooling time and are strongly dependent on the volume fraction of martensite formed during cooling, however, higher strength steels exhibit high tensile strength during lower cooling rates, due to their higher hardenability,(steel C on the Fig.1.3). During fast cooling rates, tensile strength can exceed 1200MPa when welding with low heat input.

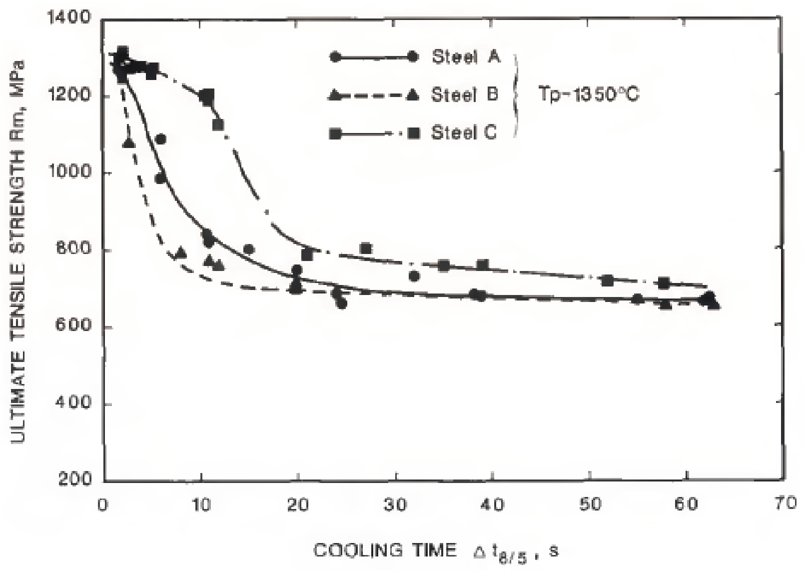

Figure 1.3: Effect of cooling time on the tensile strength of coarse-grained HAZ of three HSS (A, B and C) with Rm = 628MPa, 679MPa and 727MPa, respectively, [19]

1.2 Additional hardness analyses of HAZ

Since weld butt joint experiences diverse thermal and cooling cycles around melt zone, it may lead to differences in the mechanical properties of HAZ and rest of the material, [9], [5].
Additional Vickers hardness testing has been performed in accordance with ISO 6507-1 to support hardness results and concerns obtained from the last semester project. The utilised load used in this project is 1kg and hardness was measured on the middle line of the weld sample. Although results obtained from the last project showed some differences in hardness between weld metal and HAZ (Fig.1.4), new hardness analyses showed that no significant drop in the hardness was observed between weld metal and HAZ in both not-preheated and preheated samples, (Fig.1.5).

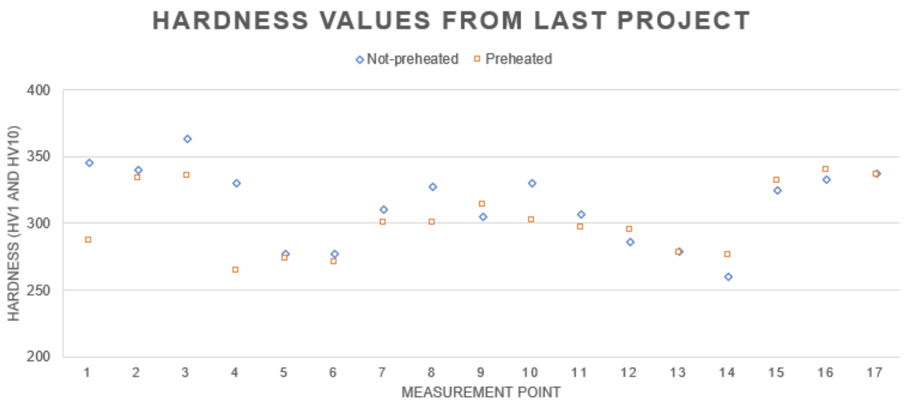

Figure 1.4: Hardness results from 9th semester's project for not-preheated and pre-heated sample

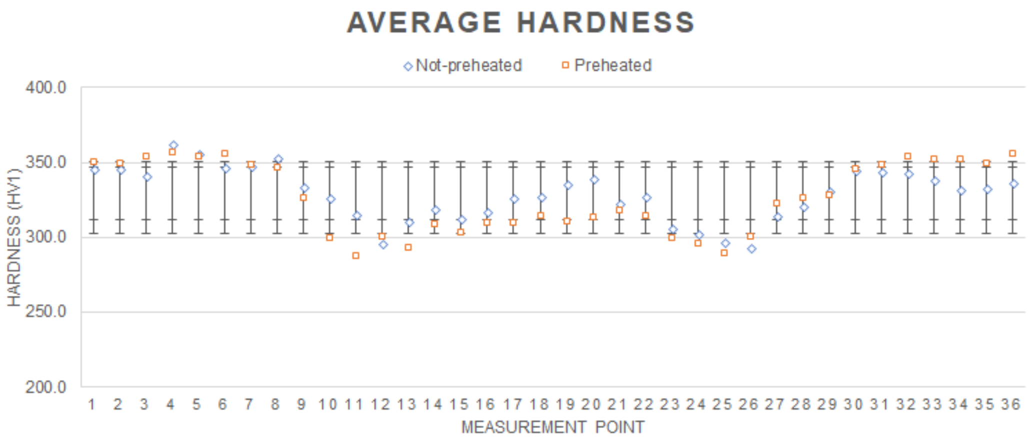

Figure 1.5: New average hardness values for not-preheated and preheated samples

In metals, micro-structural changes in the region near the fusion zone are the most important since it is the most exposed region to high peak temperatures during welding. These changes occurs as a results of thermal and cooling cycles which will be responsible for the phase transformations through HAZ and changes in mechanical properties,[9]. The hardness of a welded material usually varies noticeably through the HAZ, [13]. Khurshid and Barsoum [17] report the use of under-matched filler material to increase overall ductility of the joint. They investigated the use of matched filler material to achieve higher strength of the weld joint. It was revealed that static strength of the joint, when using under-matched filler material experiences soft layers in the HAZ as a result of heat input. Therefore, the load-deformation of the weld joint can vary with different combinations of filler material and depends on the strength of the weaker metal. The drop in the hardness of the HAZ is proposed to be due to the presence of the soft layer. However, it was found that for weld joints with matched filler and base material, soft and peak hardness were not prominent as they were for the joints with under-matched filler material.

1.3 Aim of the project

As stated at the previously, the main purpose of the project is to find how the hardness values of the HAZ are affected by the welding parameters, such as heat input and preheat temperature. Different mechanical measurements and their correlation have been introduced based on the studies made in the previous project, in section 1.1. The additional hardness measurements in section 1.2 have given a better understanding of hardness changes in the HAZ and a new approach to the problem formulation. The problem formulation of the present investigation is listed below as a set of effects that should be deeply investigated in order to provide a better understanding of effects that can cause changes in the HAZ of HSS S890QL.

Heat flow theory

The heat flow, which is applied from the welding arc, can strongly affect phase transformations during welding. It would be extremely useful to predict peak temperatures and temperature distribution in certain points outside the fusion zone in order to understand the micro-structural changes in the heat-affected base material as a result of a given heat input. The approach will be to compare analytical and experimental solutions, using heat-flow equations, in order to predict the effect of weld thermal cycles on micro-structure of HAZ.

Hardenability of steel

Jominy end quench test is used to determine the hardenability of S890QL. The hardness values at different points of Jominy sample as a function of cooling time, will be obtained. Simulations of weld thermal and cooling cycles at three different peak temperatures will be analysed and compared with micro-structural and hardness changes through the quenched sample. The hardness from the Jominy sample will later be compared to the predicted hardness model.

Prediction of maximum hardness

There have been many attempts to model the combined effects of material composition and welding parameters, such as cooling time,$t_{8/5}$, on the maximum hardness of the HAZ of low alloy steel welds. Therefore, specific empirical model will be employed and compared to the actual hardness values from the Jominy sample, as a function of cooling time. The result will be used to estimate whether a good agreement between a prediction and measured hardness of HSS S890QL will be achieved.

Chapter 2

Heat flow theory

Fusion welding has an important effect on the final micro-structure and properties of welded joints [9]. The micro-structural changes in the HAZ, are mainly affected by peak temperature and cooling rates, which are depending on the weld heat input (a function of arc energy, q , welding speed, v, and arc efficiency, η, equation2.1), thickness of the plate, and initial or preheat temperature.

$$Q = \frac{q}{v} \tag{2.1}$$

Since the changes in micro-structure due to introduced thermal cycle will affect the mechanical properties of the heat-affected base material, there is a need to characterise the thermal cycles such as peak temperature and cooling rate, in order to predict and correlate mechanical changes in the HAZ [9],[11]. The most common approach to understand thermal and cooling cycles as the results of heat input is to use Rosenthal's analytical solutions for heat flow in thick and thin plate, as described further in this chapter.

2.1 Heat flow

In the 1946, Rosenthal proposed analytical solution for the moving heat source. His approach was based on the use of complex mathematical modelling by proposing the following assumptions according to (Easterling 1983,[9]:

1. A moving heat source represents the weld arc.
2. Steady-state heat flow.
3. Thermal properties are constant with respect to temperature.
4. Heat losses throughout the surface are assumed to be negligible (this assumption is not always valid when welding thin plates).

Different experimental measurements and theoretical analyses of the weld thermal cycles have been investigated through the century. One of the analyses was carried out by

Poorhaydary et al. [11], estimating the cooling rates and peak temperatures of micro-alloyed steel Grade 690. The model have used the Rosenthal's analytical solutions for 2D and 3D heat flow with the weighting factor determined from the HAZ width. They compared the calculations with the experimental data provided by the use of embedded thermocouples in weld plates and recording thermal cycles. Moreover, thermal cycles for three different heat inputs were compared experimentally and peak temperatures and cooling rate were provided for each of the cycles.
Results from the experiment showed that higher heat input has an effect on the width of HAZ and results in higher cooling time, i.e. for the heat input of 2.5 kJ/mm welding recorded a slower thermal cycle and cooling time of 23.5s while for the lower heat input of 0.5 kJ/mm cooling time was between 1.2 and 2.6s, (Fig.2.1). This shifting of the curves to the right in the Fig.2.1 shows how cooling time drastically decreases when heat input increases. However, the experimental measurements of cooling rate showed good agreement with the predicted one.

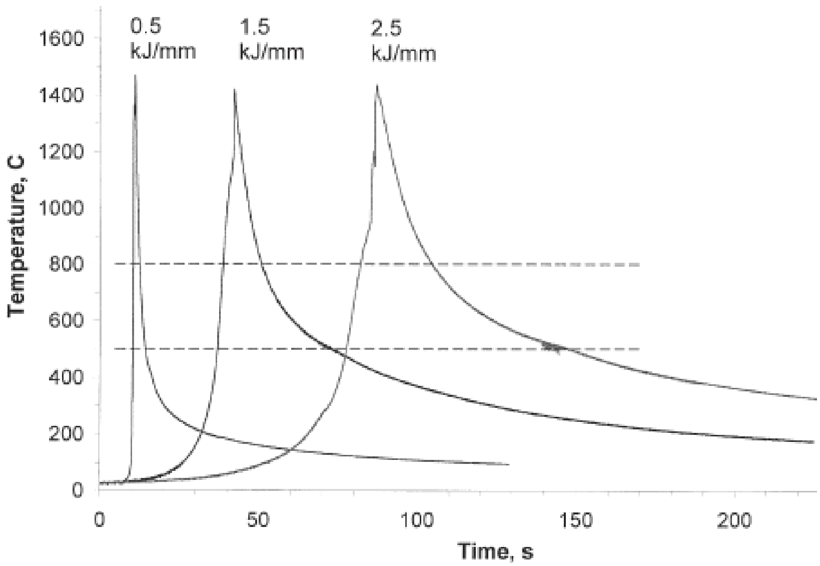

Figure 2.1: Effect of different heat inputs on the cooling rates, [11]

In the next research, Easterling et al. [12], as well used Rosenthal's equations to predict the micro-structure of the real weld of micro-alloyed high strength steels. Rosenthal's equations provides an overview of the time-shape of thermal cycle peaks. In order to check the validity of the constructed HAZ diagrams using the results from the simulated welds they drilled the wholes in the HAZ, embedded thermocouples and measured the temperature-time cycles. The results showed the relation over a wide range of energy inputs, between calculated Rosenthal's equations for the thick plates and actual thermal cycles measured in the real welds.
In the first report, Ashbi and Easterling, [3], used Rosenthal equations to estimate the temperature profiles and grain growth of six different micro-alloyed steels. The results

again showed a good relation between real and simulated weld. They found that preheat temperature and input energy highly affect the structure of the HAZ.
Numerous other attempts to explain the relations between the real and simulated welds have been made. In general, results appear to be satisfactory with respect to both, micro-structure and mechanical property measurements. The thermal cycles obtained from Rosenthal equations are programmed in weld simulation and the final micro-structure depends mainly on the completed thermal cycle. However, the possible differences in the micro-structure can appear, such as differences in cooling and heating rate. Nevertheless, good agreements between predicted and actual thermal cycles in Rosenthal equations can usefully describe the effect of arc-welded thermal cycles on the changes in the micro-structure of HAZ, [9], [13], [12].

2.2 Rosenthal's equations

The temperature distribution and cooling rates outside the weld pool can be determined using a Rosenthal's theoretical model by applying the theory of a heat transfer respect to moving heat source during welding, [13].
This solution provides the temperature distribution in the quasi-stationary state by using a co-ordinate system (x,y,z), which moves at a same speed **v** as the welding arc, along the x-axis as shown in the Fig.2.2.

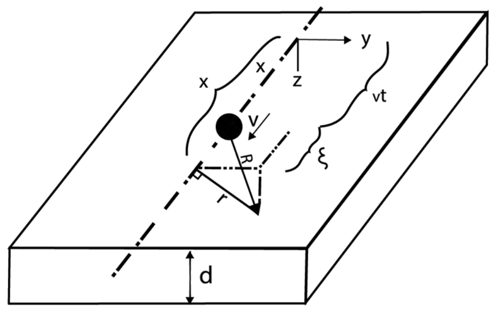

Figure 2.2: Rosenthal's moving co-ordinate system in a terms of heat source

If the heat is supplied to the weld with a constant speed, the quasi-stationary state can be achieved if the variable ξ is defined as $\xi = x - vt$, as the distance from the origin heat point to the specified point along the x-axis and if the temperature distribution around this specific source is constant in respect to the time, which can be expressed by constant form, $\frac{\partial T}{\partial t} = 0$, which gives:

$$\frac{\partial^2 T}{\partial \xi^2} + \frac{\partial^2 T}{\partial\, y^2} + \frac{\partial^2 T}{\partial\, z^2} = -\frac{c\rho}{\lambda} \upsilon \frac{\partial T}{\partial \xi} \tag{2.2}$$

where T is temperature, t is time, λ is thermal conductivity and ρc is heat capacity. During fusion welding, the flow of heat from the source mainly depends on the thickness of the plate and therefore can be conducted radially for the thick plates or laterally for the thin plates, through the material.
Equation 2.2, served as a basis for the Rosenthal's two main solutions for three-dimensional (3D) and two-dimensional (2D) heat conduction problems in welding, respectively. Fig.2.3 schematically shows both conditions and despite the Rosenthal's assumption about negligible heat losses on the surface in real welds, the heat flow when welding thin plates will be dissipated through the surface of the work-piece.

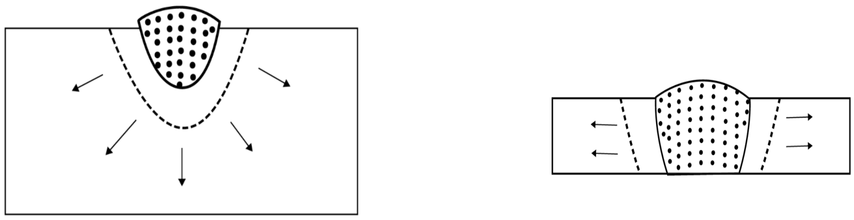

(a)

(b)

Figure 2.3: hree and two dimensional heat flow in welding, [9]

The three-dimensional Rosenthal's equation is given by Eq.2.3. The radial distance from the weld line to any specific position in the work-piece is given by r, where $r^2 = z^2 + y^2$, (Fig.2.2). The exponential part in the Eq.2.3 controls the rapid heating and reverse part controls the cooling phase of the curve.

$$T = T_0 + \frac{Q}{2\pi\lambda t} exp\left(\frac{-r^2}{4at}\right) \tag{2.3}$$

Where	T	Temperature in the material
	T_0	Initial temperature in the material before welding, e.g.preheating temperature.
	Q	Specific heat input.
	λ	Thermal conductivity.
	t	Time in seconds.
	r	Radial distance from the weld center.
	a	Thermal diffusivity, given by$a = \frac{\lambda}{\rho c}$.
	ρc	Thermal capacity.

Since time(t) occurs in the Eq.2.3, heat-affective zone experiences thermal cycle as function of temperature and time, Fig.(2.4).

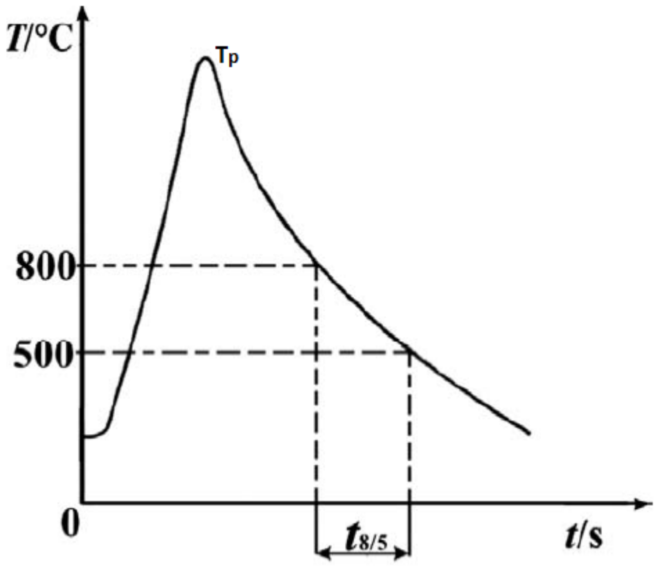

Figure 2.4: Schematic representation of weld thermal cycle as a function of time

The cooling time, Δt_{8-5}, represents the time needed for the HAZ to cool down from the temperature range of 800-500 $°C$ and has an effect on the micro-structure of the weld joints, [9]. For a given welding process, material type and geometry, the cooling time,Δt_{8-5}, is constant, at least for the heat-affective base material where peak temperature is higher than 900 $°C$, and it can be calculated from the Eq.2.4 as:

$$\Delta t_{8-5} = \frac{Q}{2\pi\lambda}\left(\frac{1}{500 - T_0} - \frac{1}{800 - T_0}\right) \tag{2.4}$$

It should be noted that Δt_{8-5} is completely independent of the distance from the heat source, [15], [9].

The peak temperature at any given position from the fusion zone can be analytically calculated and can be written as,[13],[9]:

$$T_p = T_0 + \left(\frac{2}{\pi e}\right)\frac{Q}{\rho c r^2} \tag{2.5}$$

Equation is applicable to single-pass processes and should be applied to each pass individually. It can be also used for evaluating the size of heat-affective zone and to show the effect of preheat on the HAZ size,[14]. This is important because in the multi-run welds each subsequent thermal cycle effects the part of the previous weld run. Nevertheless, this results in improvement in toughness and refinements of micro-structure, [9],[13].
In two-dimensional heat flow, temperature-time distribution can be calculated by following the equation 2.6, where z-coordinate is ignored, and the thicknes d is used directly since 2D solution depends on this parameter,[15].

$$T = T_0 + \frac{Q}{d(4\pi\lambda\rho c t)^{\frac{1}{2}}} exp\left(\frac{-r^2}{4at}\right) \tag{2.6}$$

Where	T	Temperature in the material
	T_0	Initial temperature in the material before welding, e.g.preheating temperature.
	Q	Specific heat input.
	d	Thickness of the plate.
	λ	Thermal conductivity.
	t	Time in seconds.
	r	Radial distance from the weld center.
	a	Thermal diffusivity, given by $a = \frac{\lambda}{\rho c}$.
	ρc	Thermal capacity.

Since heat flow might have two or three-dimensional features, the Eq.2.7 is used to calculate the transition thickness,d_t, over which the boundry between 2D or 3D is defined,[20], [9]. It should be noted that transition thickness is only dependent on the material thickness, heat input and preheat temperature,(Fig.2.5).

$$d_t > \left[\frac{Q}{2\rho c}\left(\frac{1}{773 - T_0} + \frac{1}{1073 - T_0}\right)\right]^{\frac{1}{2}} \tag{2.7}$$

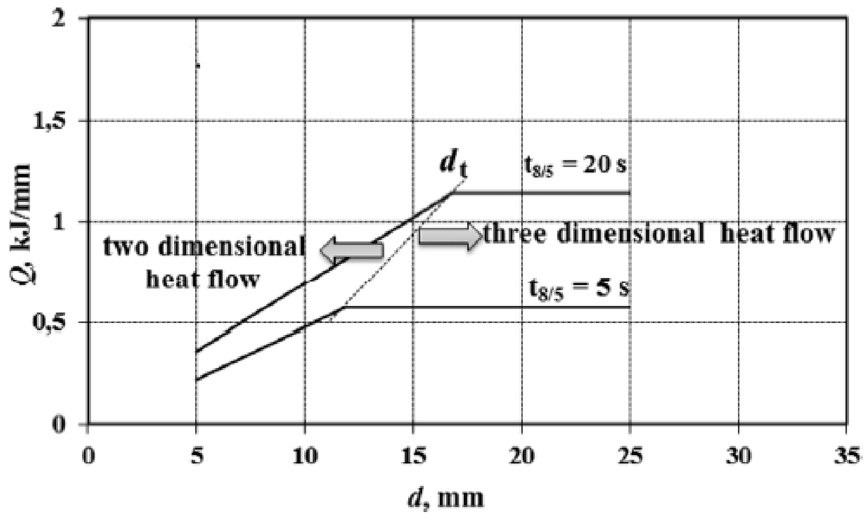

Figure 2.5: The relationship between transition thickness and heat input, [20]

The main idea was to use the transition thickness, equation(2.7),to evaluate the actual state of heat flow, whether 2D or 3D, to explain actual response of welded joint to the thermal cycle. Therefore, based on the Eq.2.7, and using the material parameters, the transition thickness is calculated. With heat input of 0.9 kJ/mm and plate thickness,d=15mm, it was decide to use the 3D state of heat flow.

Thermal modelling

All the equations used for thermal modelling are stated in the part for Rosenthal's solutions. The equations and thermal properties for carbon steel are gathered from (Easterling,[9]). Thermal properties values are refereed to the data for the carbon steel reported in the (Easterling,[9]). For the first simulation, following conditions were used in the Eq. 2.3 and Eq. 2.5

Initial temperature, $T_0 = 295K$
Heat input,$Q = 0.9KJ/mm$
Thermal conductivity, $\lambda = 41J/msK$
Distance, $r = 5mm, 5.5mm, 8 = mm, 11mm$
Thermal diffusivity, $a = 9.1 \times 10^{-6}$
Thermal capacity, $\rho c = 4.5 \times 10^6$

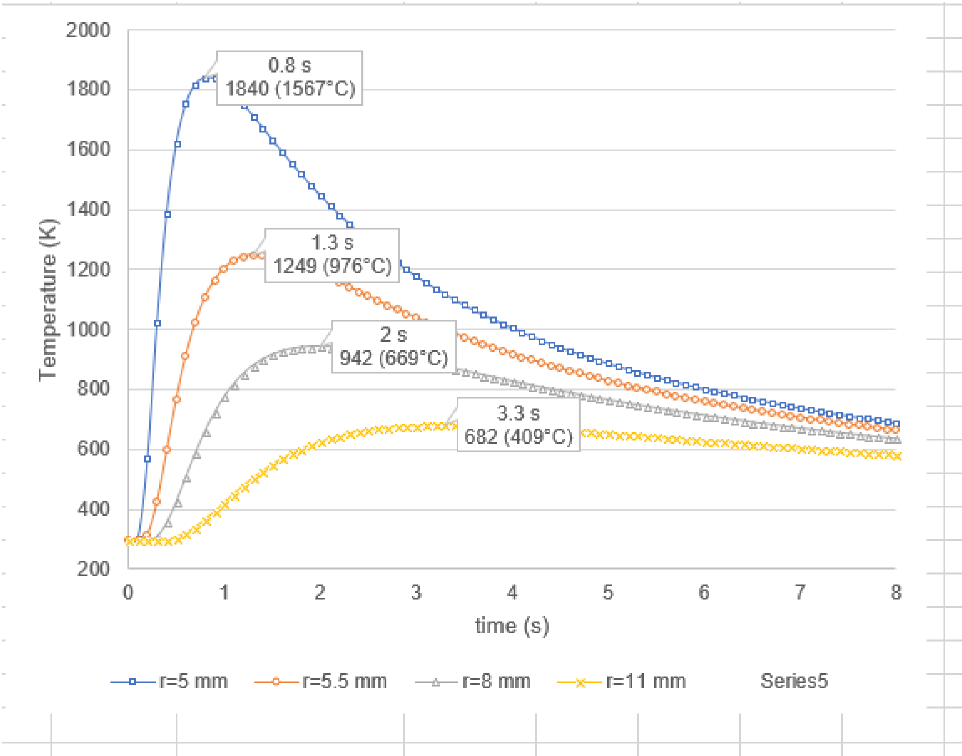

Figure 2.6: Temperature versus time profile for the material with initial temperature,$T_0 = 295K$.

Temperature-time profile for a thick plate model with a $T_p = 295K$, at Fig.2.6, gives the thermal cycles throughout the HAZ as a function of time for four different (r) positions. The time required to reach the peak temperature decreases with increasing distance from the center line. Moreover, both the heating and cooling rate decrease with increase the distance.

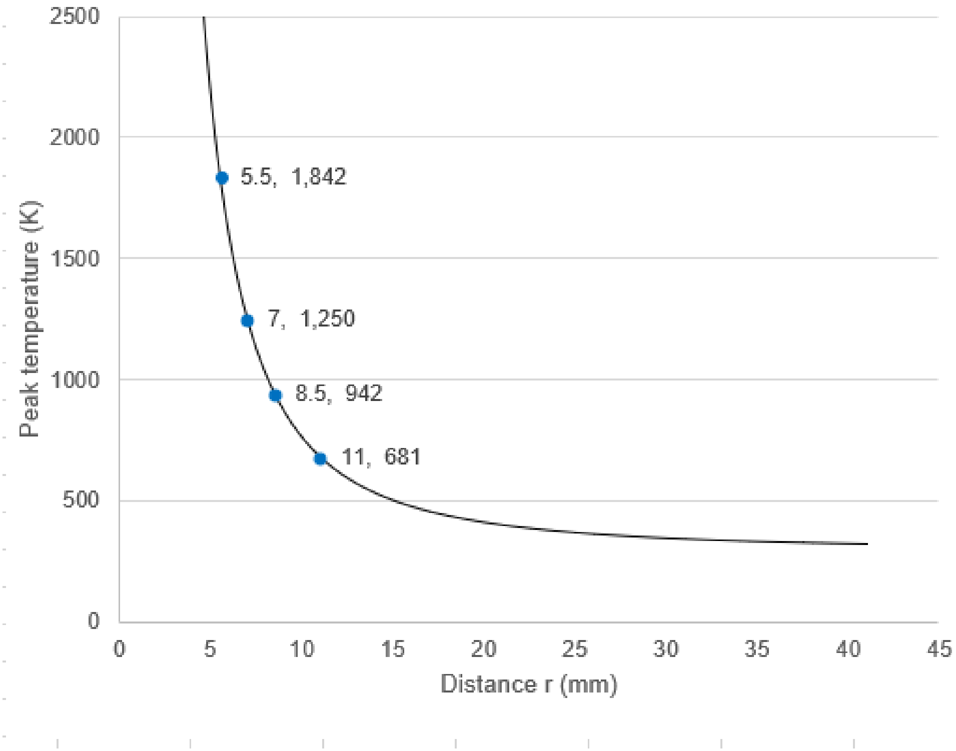

Figure 2.7: Peak temperature as a function of distance from the weld center,$T_0 = 295K$.

Rosenthal			Peak T			Error
Time (s)	T (K)	T (°C)	Distance (mm)	T (K)	T (°C)	
0,8	1840	1567,2	5,5	1842	669	0,09 %
1,3	1249	976	7	1250	1077	0,07 %
2	942	669,3	8,5	942	762	0,05 %
3,3	681	408,5	11	681	681	0,09 %

Table 2.1: Results obtained for the first simulation for the material with initial temperature, $T_0 = 295K$

The behaviour of the peak temperatures versus four different positions from the weld center (see Tab.2.1) are plotted in the Fig.2.7. The figure shows that peak temperature rises to infinity when approaching the heat-source. Moreover, the slope of rapid decrease as a function of distance is quite expressed.
Therefore, the Rosenthal method approximates the welding conditions and describes the relationship between the heat input,Q, and preheat treatment,T_0, on the peak temperatures,T_P and cooling time,Δt_{8-5}. The importance of it is because. This is

important because if using this information, the prediction of metallurgical transformation can be done. This will be explained by the 3D simulation graph in the Discussion chapter.

Chapter 3

Hardenability of steel

The knowledge of thermal and cooling cycles for the materials such as steels is important since they experience the formations of different phases. To predict which micro-structural change will occur during cooling, various heat treatments have been developed,[6].

Heat treatment of steels

In general, heat treatments are used to optimize the properties of a steel by producing a steels with high content of martensite, [7], [21]. To achieve this, process involves continuous and rapid cooling of an austenitized specimen by water, oil or air. The factors that are determining whether a heat treatment will produce fully martensitic micro-structure, are the composition of the alloy, the type of quenching and the size and thickness of the sample, [7].

Hardenability

For every different steel alloy there is a certain relationship between the mechanical properties and cooling rate, [7]. The ability of the steel to transform to martensite during quenching from the high temperatures corresponds to its hardenability. However, hardenability is not related to the hardness of the martensite but to the depth to which martensite can be produced, [21], [7].
The procedure used to determine the hardenability of the steel is the Jominy end quench test. This test is used to measure the capacity of the steel to be harden in depth under give set of conditions. The results from the Jominy test can be used to determine the changes in cooling time as a function of distance from the quenched end. This changes in cooling time will result in different formation of micro-structure along the Jominy sample. The quenched end is cooled most rapidly and will produce a micro-structure with 100% of martensite. However, with the distance from the quenched end, the cooling time decreases while hardness values decreases, beacuse of the decreased amount of martensite in the formed micro-structure, [21], [13].

3.1 Transformations during cooling

Figure 3.2, shows the micro-structure changes after cooling of S890QL steel. The base metal consists of tempered martensite. The HAZ micro-structure can be divided into essentially three regions: partially transformed, normalised or grain refined,and coarse grained zone,(Fig.3.1). The peak temperatures for the each position of the zones is indicated on the phase diagram,(Fig.3.1:**(b)**).

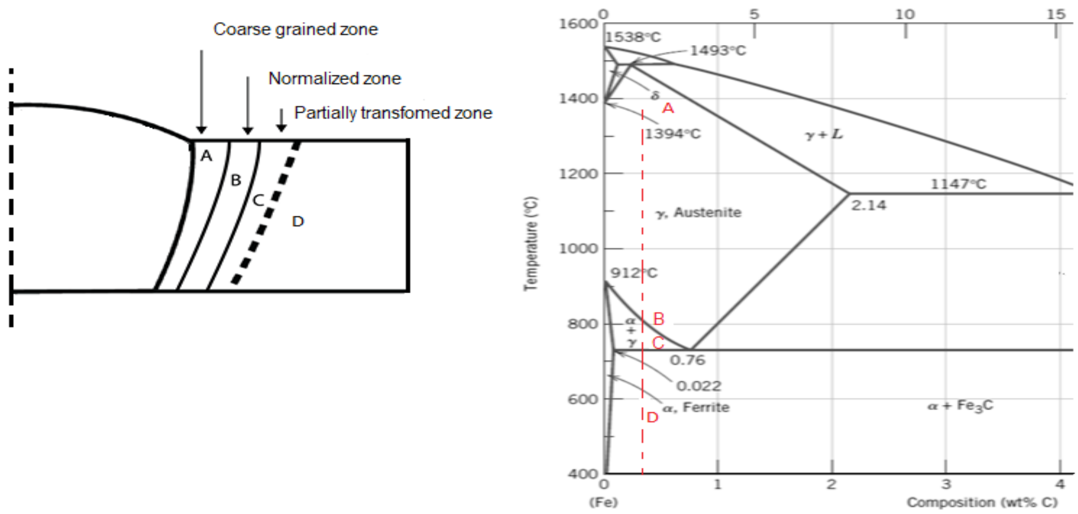

(a) **(b)**

Figure 3.1: Different regions in HAZ **(a)** Shematic representation of butt weld joints. **(b)** Phase transformation diagram for iron-carbon alloys, [7]

The type and volume fracture of new transformed phase depends on various factors, such as grain size, cooling rate, peak temperature, content of alloying elements and similar,[9],[13],[21].

Partially transformed zone corresponds to the temperatures range from $750 - 900°C$ in the $\alpha - \gamma$ region,(point C on the Fig.3.1:**(b)**). Upon heating, pearlite colonies transforms to austenite(γ) and then upon cooling change back to fine small graines of pearlite and ferrite(α). Furthermore, the prior ferrite colonies does not change phases during heating or cooling,[7],[9]. It should be noted that this transformation happens for the unalloyed low-carbon steels. Formation of micro-structure for low alloyed carbon steels will mainly depend on the alloy content and the cooling rate, [13],[9]. Therefore, the $\alpha \rightarrow \gamma$ transformations upon rapid cooling can be transformed into other phasese, such as tempered martensite. This phase transformations are likely to be present in low alloyed high strength steel, S890QL (Fig.3.2;**(c)**).

Normalised or grain-refined zone,(3.2), is subject to lower γ-phase temperature region, $900 - 1100°C$, (point B on the Fig.3.1:**(b)**). As a results of lower peak temperatures, austenite, upon heating does not have time to transform properly which can result

in very small grains. Upon cooling, such small austenite grains decompose into small pearlite and ferrite grains depending, of course, on the cooling rates, alloying content of the steel, etc,[9],[21]. Furthermore, the distribution of ferrite-pearlite structure is usually not uniform, since ferrite will start to nucleate at the large grain boundary area while pearlite grains will form at the center of the grain which is rich in carbon,[13]. For the low alloy carbon steels, depending on the cooling rate, grain-refined zone is most likely to transform to martensite or upper bainite, (3.2:**(b)**).
Coarse-grained heat affective zone is subjected to a high γ-phase temperature region, up to 1400°C, (point A on the Fig.3.1:**(b)**). High heat temperatures allows formation of large austenite grains. Upon larger cooling there is a tendency for the ferrite to grow from the grain boundries as side plates, so called Widmanstatten ferrite, [8].Although, in low-carbon steels, martensite phases are normally not observed, upon high heating and cooling rates it is possible that marteniste will be formed and result in hard and brittle HAZ, [9], [8].

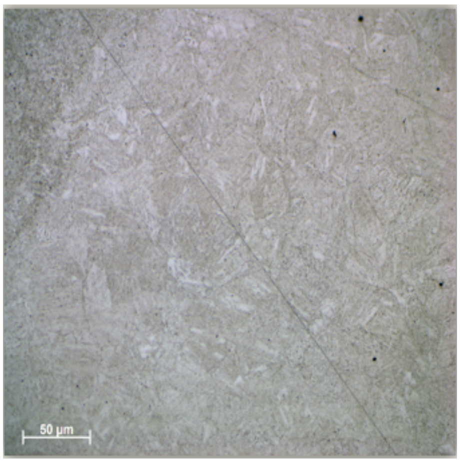

(a)

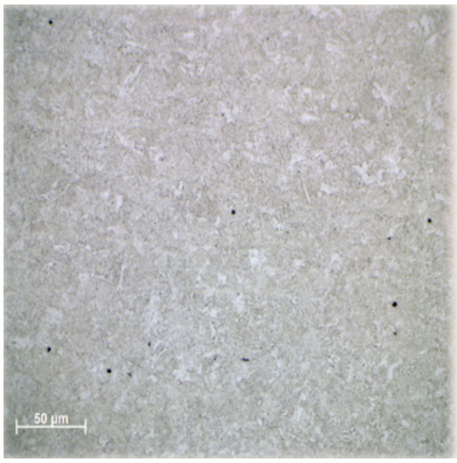

(b)

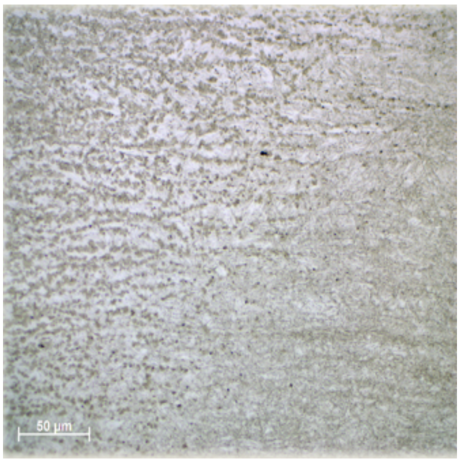

(c)

(d)

Figure 3.2: Different regions in HAZ of S890QL steel **(a)** Coarse grained zone **(b)** Grain refined zone **(c)** Partially transformed zone **(d)** Base material

Chapter 4

Hardness prediction model

The hardness of a welded material usually varies noticeably through the HAZ, [13]. The properties of a welded joint are a sensitive function of micro-structure as a result from the welding cycles. Safe welding procedures are designed on maximum HAZ hardness resistance to cold cracking and controlled by carbon equivalent and cooling time $\Delta t_{8/5}$, [16]. For low alloyed steels the maximum hardness,(H_{max}), is most often found in the coarse grained zone, where both the heating and the cooling rates are very high, [13], [4]. Formation of martensite upon fast cooling is often associated with an increase in hardness. Higher hardness levels can also indicated that duccility of the HAZ in comparison to base material decreased. A numerous equivalent formulas and maximum hardness prediction models have be noted.

Review of different hardness prediction models

Different hardness prediction models have been made in order to predict the maximum hardness in the HAZ as a function of cooling rate, for the specific type of steel, [11], [4], [15], [12].
Borggreen [4], has made a review on four essential different analytical approaches to describe the hardness curves. The Lorenz-Dulen, Suzuki, Yurioka and Terasaki model have been used to describe the (H_{max}) hardness as function of coolint time, Δt. Arata model have been used to predict the micro-structure.
The Lorenz-Duren model have proposed a formula (Eq.2.6), for evaluating the maximum HAZ hardness.

$$H_{max} = 2019 \cdot (1 - 0.5log\Delta_{8/5})C + 0.3 \cdot (CE_B - C) + 66 \cdot (1 - 0.8log\Delta_{8/5}) \tag{4.1}$$

where

$$CE_B = C + \frac{Si}{11} + \frac{Mn}{8} + \frac{Cu}{9} + \frac{Cr}{5} + \frac{Ni}{17} + \frac{Mo}{6} + \frac{V}{3} \tag{4.2}$$

The Lorenz model is more applicable for the steels with carbon contente, $C > 0.18\%$

and for $\Delta t_{8/5} > 12s$.
The maximum hardness curve in the Yurioka model is described in Eq.2.5, with the use of arc tangential curve:

$$H_{max} = \frac{(H_{M100} + H_{M0})}{2} - \frac{(H_{M100} - H_{M0})}{2.2} \cdot arctanX \tag{4.3}$$

where X is function of carbon equivalent and cooling time. Yurioka model is more valid for the steel with $C < 0.22\%$ and for $\Delta t_{8/5} < 6s$. However, since this model only relies on the volume of martensite fraction, which for the very high and low cooling rates can not be inaccurate, since formation of other constituents can be expected, [4].
Kakhki et al. [16], in order to calculated the hardness of martensite, bainite, pearlite and ferrite as a function of chemical composition and cooling rate. The total hardness of a steel was calculated using the rule of mixture:

$$HV = F_M HV_M + F_B HV_B + (F_F + F_P) HV_{F+P} \tag{4.4}$$

where HV is the total hardness of particular steel in Vickers.
Lundberg, [15], as well used the rule of mixture to calculate the hardness in HAZ. In his studies, he relies on the relation between the carbon content and hardness of the individual phases. The maximum hardness is then possible to calculate by a rule of mixture:

$$H_{max} = V_m H_m + V_b H_b + V_{fp} H_{fp} \tag{4.5}$$

Important for note is that when evaluating the hardness in the HAZ, these approach is applicable for the steels with a carbon content, $C < 0.5\%$.

4.1 Terasaki model

The Terasaki model is applicable for mild steels as well for the low alloy steels and,therefore, have been employed to predict the maximum hardness in the HAZ for the low carbon alloyed S890QL steel.
The Terasaki model estimates the hardness limit of martensite by follow equation:

$$H_{max} = H_M \tag{4.6}$$

if

$$\Delta t_{8/5} < \Delta t_M \tag{4.7}$$

$$H_{max} = H_\infty + (H_M - H_\infty) \cdot exp(-0.2(\Delta t_{8/5} - 1)) \tag{4.8}$$

if

$$\Delta t_{8/5} > \Delta t_M \tag{4.9}$$

where Δt_M is the cooling time giving 100% martensite, (see Fig.4.1. The formula used to calculate the carbon equivalent,Pv, is:

$$Pv = C + \frac{Mn}{3} + \frac{Cu}{4} + \frac{Ni}{8} + \frac{Cr}{10} + \frac{Mo}{3} + 5B \tag{4.10}$$

where $log\Delta t_M = 2.5Pv - 1.27$.
Hardness,H_{M100} for the 100% martensitic micro-structure can be written as Eq.4.11, while the hardness, H_{M0}, for 0% martensite can be expressed by Eq.4.12.

$$H_M = H_{M100} = 812C + 293 \tag{4.11}$$

$$H_\infty = H_{M0} = 164 \cdot (C + \frac{Si}{2} + \frac{Cr}{2} + \frac{Mo}{2} + V + Nb + 7B) + 153 \tag{4.12}$$

The empirical method for Terasaki model was employed (Fig.4.1) by using the chemical composition (Tab.4.1) and cooling time,$t_{8/5}$, to generate the predicted hardness value, and this was compared to the measured hardness data, which is present later in the result section.
The Fig.4.1 shoes how predicted hardness varies with increasing cooling time for a given chemical composition).

Chemical composition %							
C	*Si*	*Mn*	*P*	*S*	*N*	*Cu*	*Mo*
0.165	0.28	0.88	0.008	0.001	0.005	0.028	0.51
Ni	*Cr*	*V*	*Nb*	*Ti*	*B*	*Zr*	*Al-T*
0.52	0.48	0.045	0.01	0.002	0.0002	0.0002	0.034

Table 4.1

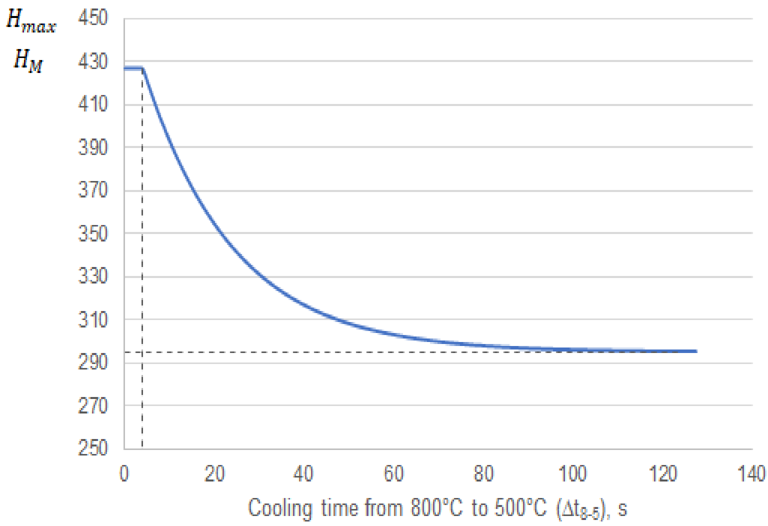

Figure 4.1: The calculated maximum hardness curve according to Terasaki model

Chapter 5

Method, results and discussion

5.1 Methodology

5.1.1 Experimental set-up

The initial thickness of the material was smaller than 25,4mm and 102mm (according to standards), modifications were made. With a help from the lab technicians, the Jominy sample were suppresed in the metal tube with diameter of 25.4mm, as you can see from the Fig.

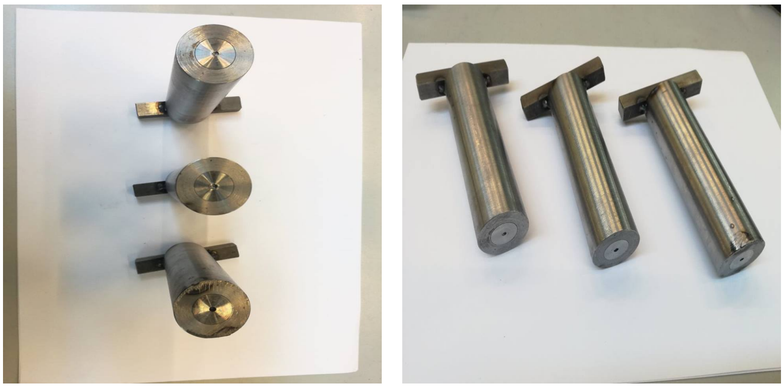

Figure 5.1: The modificated Jominy sample (the tested material is inside the metal tube)

5.1.2 Procedure

Heating

Three Jominy bars were used in this experiment. The heat treatment process had two stages. Three Jominy samples were heated up to 700°C, 900°C and 1150°C. The first stage was heating the metal to a desired temperature 700°C, 900°C and 1150°C

and then cooled down to the room temperature by water. Moreover, before the real heating and cooling process started, the Jominy test sample was used in order to ensure that proper heat measurements will be applied when the real experiment starts. The furnace took half an hour to get up to $750°C$. Furnace was heated $50°C$ higher than the needed temperature in order to ensure that temperature of the sample is above the desired temperature after the sample is taken out from the furnace. The length of each heat cycle was measured by the use thermocouple placed in the middle of sample. The other end of the wire was attched to thermologger, in order to ensure the proper time needed to put the sample out of the furnace and begin the quenching process.

Quenching

The quenching process was the same for the each sample. The sample was taken out from the furnace and placed into apparatus that was placed closed to the furnace. The step between taking the sample out of the furnace and positioning it on the quench apparatus should be completed in very short time to avoid that ambient air temperature cool down the sample. To insure that the right distance between the water spout and the sample, small rectangle bar was welded to the opposite end of the each sample. This ensured the water spout properly quench the bar. The samples took two to four minutes to change from bright to black, Fig.5.2. When the samples were cooled down to a room temperature, they were labelled and saved into bags.

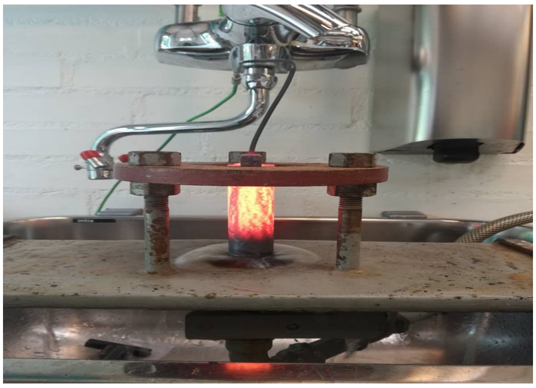

Figure 5.2: The modificated Jominy sample (the tested material is inside the metal tube)

Machining

Upon cooling the bars were taken to be machined. First, the samples were cut into two pieces, the part that was quenched was cut again into two parts, as you can see from the Fig.5.3. One half for each sample was grinded and electro-polished and later used for the metallographic examination while another half was used to performed hardness measurements. Metallographic examination and hardness measurements were performed along the cylinder axis as a function of distance from the quenched end. The hardness measurements were performed by using a Vickers diamond of 1kg. The micro-structure of each sample was observed using an optical microscope.

Figure 5.3: The modificated Jominy sample (the tested material is inside the metal tube)

5.2 Results and discussion

5.2.1 Rosenthal modelling

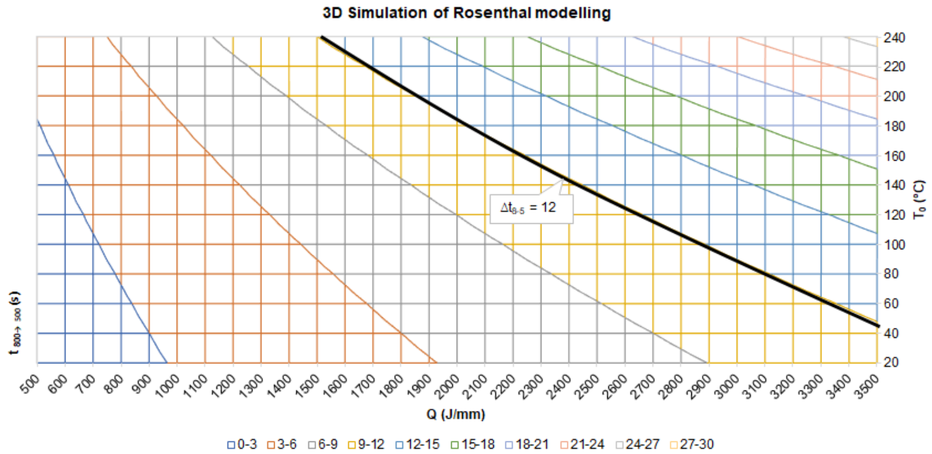

Figure 5.4: 3D Simulation of Rosenthal modelling with relation between heat input,(Q), peak temperature,(Tp) and pre-heat treatments,(PT)

As already analytically demonstrated in the Chapter 2 (see Fig.2.7 and 2.6), the further the distance from the welding zone, the value of the peak temperature is decreasing. The effect on the heat input,(Q), and pre-heat treatment,(PT), on the increase of the cooling time,$\Delta t_{8/5}$, is shown in the 3D Rosenthal simulation on the Fig.5.4. The model shows that the pre-heated sample, the heat input will have significant effect on the cooling time,$\Delta t_{8/5}$, in comparison to the not-preheated sample. According to recommendations from the suppliers of the S89QL steel, the welding conditions should be chosen so that the cooling time $t_{8/5}$, does not exceed 12s. This can be controlled if a right combination of the heat input,Q, and preheat temperature,T_0, is used. Therefore, the analysis conditions to see the effect in the cooling time for preheated and not-preheated where chosen as for the preheated and not-preheated material, with low heat input of 900 J/mm and with initial temperature of $130°C$ and $22°C$, respectively. In both cases, the weld joints provided astounding properties regarding toughness, tensile strength and hardness.

It is concluded that proper preheating helps to slow the cooling time of the finished weld and reduce hardness in the HAZ which can create weld which is less brittle and more ductile. When the cooling time is slower, it gives more time to form less brittle but more ductile micro-structure. The effect of the cooling time on the micro-structural changes is characterise in the Jominy section. Various mechanical testing confirmed that high strength S890QL steel which was not exposed to any preheat treatments, exhibited equally high toughness as well as tensile strength and hardness in comparison to the preheated S890QL steel. This results can help in design and better understanding of the materials behaviour. Moreover, it is one step less in the welding process which can save time and costs when manufacturing high strength steels.

5.2.2 Jominy simulations

The Jominiy test was performed as described in the methodology section, using Jominy test specimens, quenched from three different austenite temperature, $700°C$, $900°C$ and $1150°C$. Hardness measurements are then taken along the bar and plotted as a function of distance. The results from Jominy experiments will be plotted for each austenite temperature. Temperature-time graph and hardness graph will be discussed and compared to a micro-structural changes obtained during quenching.

Jominy test sample quenched from $700°C$

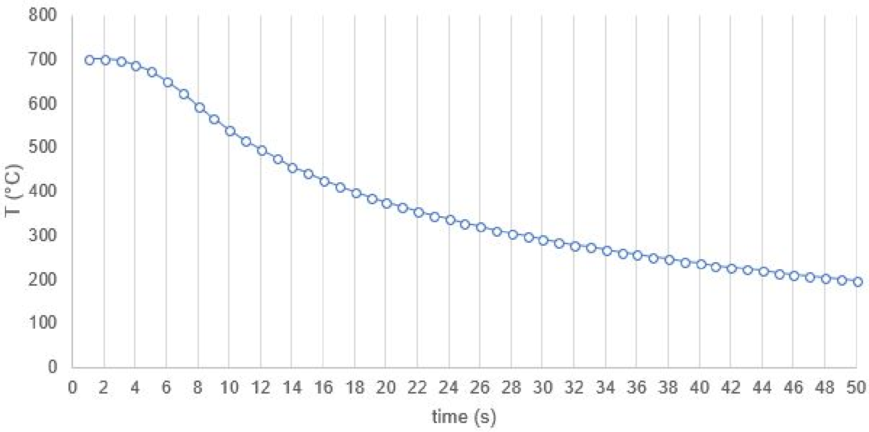

Figure 5.5: Temperature versus time for the Jominiy sample quenched from $700°C$ at r=11mm

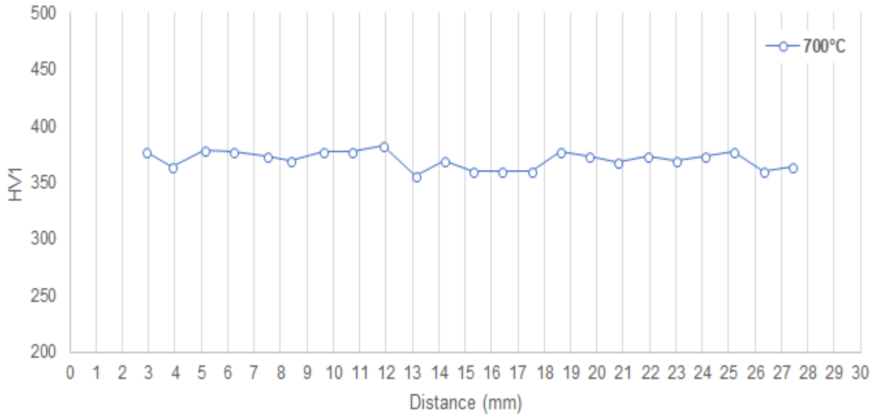

Figure 5.6: Hardness measurements for the Jominy sample quenched from $700°C$ as a function of distance from the quenched end

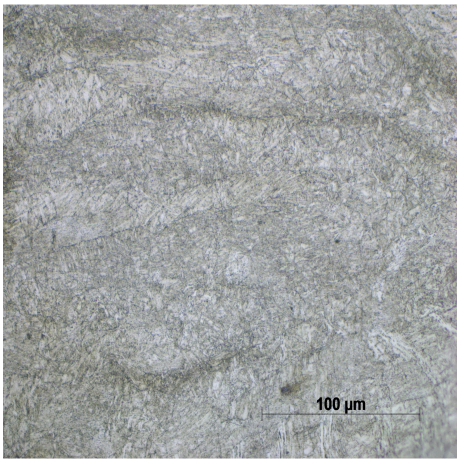

(a)

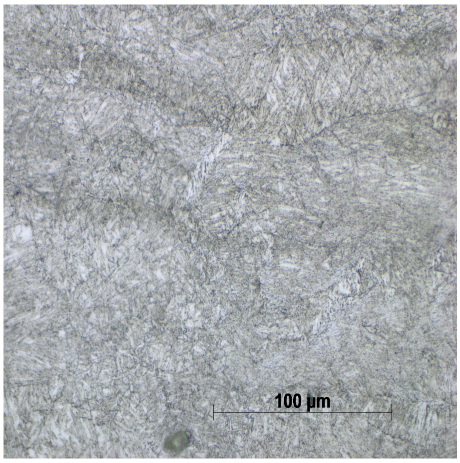

(b)

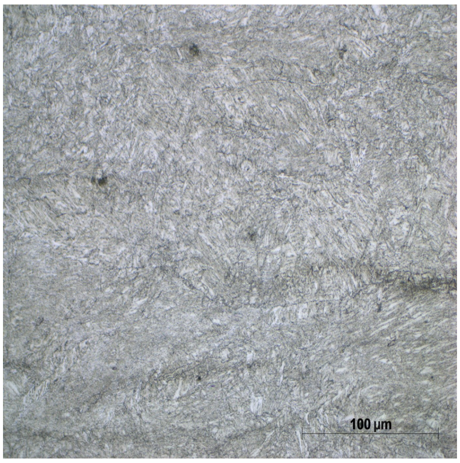

(c)

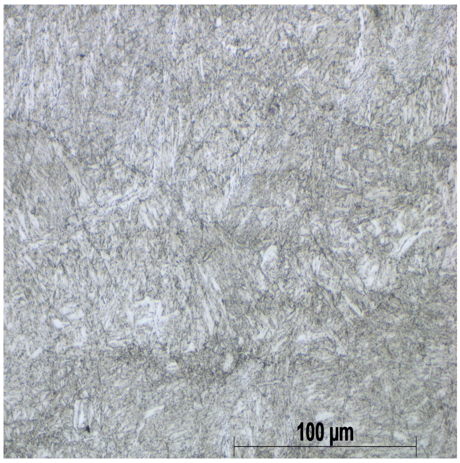

(d)

Figure 5.7: Different micro-structures of Jominy sample with $T_P = 700°C$ as a function of distance **(a)** 0.3 mm from the quenched end **(b)** 3mm from the quenched end **(c)** 5mm from the quenched end **(d)** 11mm from the quenched end

The curve at Fig.5.5 represents the time needed to cool down the Jominy bar from $700°C$ to room temperature. Although, the cooling time increases gradually with increase in distance from the quenched end, the Jominy sample experienced equal hardness distribution through its entire length, as it can be seen from the Fig.5.6. In general, changes in morphology at temperatures below $700°C$ do not occur, [9]. Since hardness values does not exceed 400HV, the micro-structure formation is proposed to be tempered marteniste, (see Fig.5.7). This type of micro-structure is result of tempering which is carried out at this temperatures and this micro-structure is much more stronger and tougher than the brittle marteniste, [7].

Jominiy test sample quenched from $900°C$ and $1150°C$

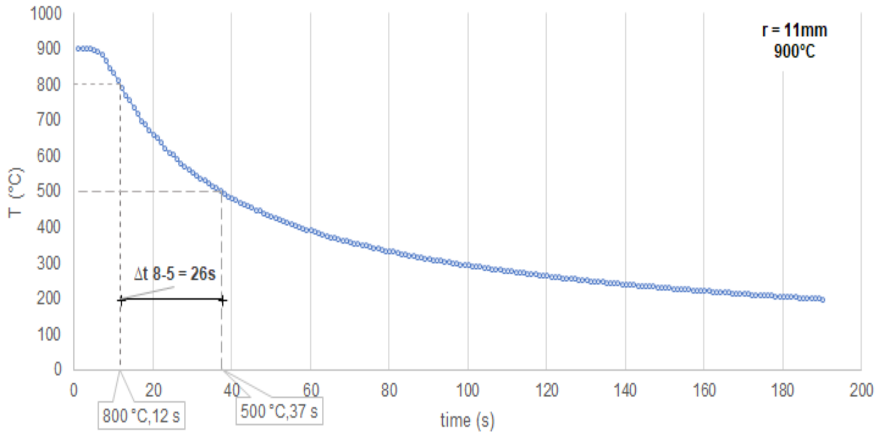

Figure 5.8: Temperature versus time for the Jominiy sample quenched from $900°C$

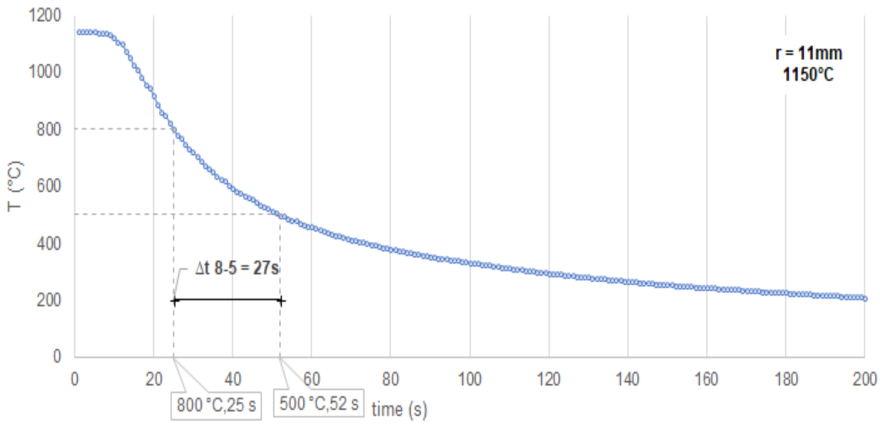

Figure 5.9: Temperature versus time for the Jominiy sample quenched from $1150°C$

Figures 5.8 and 5.9 are showing the temperature-time profiles for the Jominy sample with $T_P = 900°C$ and $\Delta t_{8-5} = 26s$, and $T_P = 1150°C$ and $\Delta t_{8-5} = 27s$, respectively, at 11mm from the quenched end. During cooling a Jominy sample from its solidification temperature, $T_P = 900°C$ and $T_P = 1150°C$, to the ambient temperature, different transformation in micro-structure have ccurred, (see Fig,5.11 and 5.14). The cooling time, Δt_{8-5} is determining factor in the resulting micro-structure, [15], [9]. Although, the decrease in the temperature in the Fig.5.8 is more rapid than for the Jominy sample with $T_P = 1150°C$, the cooling time, Δt_{8-5} is relatively slow for both Jominy sample. However, this is the case for the distance 11mm from the quench end. The Fig5.10 is showing the relation between the cooling time, Δt_{8-5}, as a function of distance from the quenched end at four different positions.

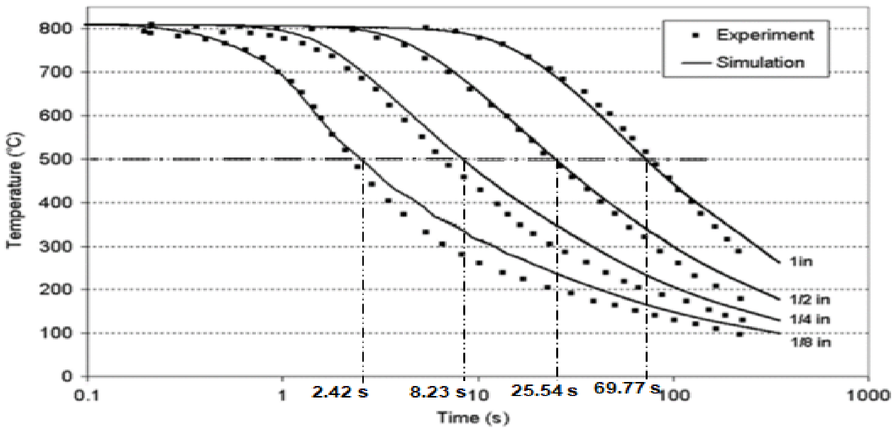

(a)

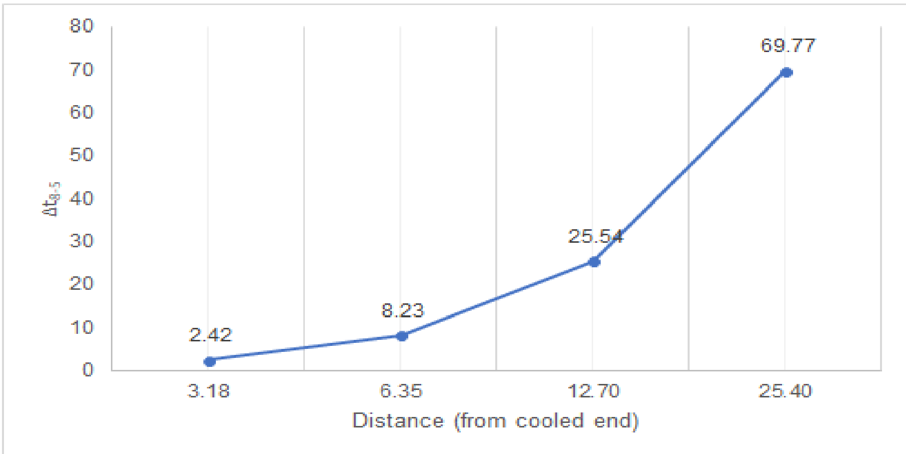

(b)

Figure 5.10: Cooling time versus distance from the quenched end **(a)** Cooling time vs. distance **(b)** Temperature-time profiles for the Jominy sample cooled from 800°C, [16]

It should be noted that this data were extrapolated from the Jominy experiment made on the low alloy high strength steel 4140 grade, [16]. Kakhi et al. made a model predictions and the measured temperature histories on the points located at distances 3.18mm(1/8in), 6.35mm(1/4in), 12.70(1/2in) and 25.40mm(in) from the quenched end of the Jominy sample(see Fig.5.10). The comparison is made only with a Jominy sample with $T_P = 900°C$.
The cooling curve from the Fig.5.10:**(a)**, at 12.7mm(1/2in), describes quite similar behaviour of the cooling process in the Fig.5.8, at 11mm from the quenched end, measuring the cooling time, Δt_{8-5}, 25.4s and 26s, respectively. Furthermore, by using this approach, the cooling time,Δt_{8-5}, vs. distance, from the Fig.5.10 will be used further to describe the effect of the cooling time,Δt_{8-5}, on the micro-structure changes along the Jominy sample at four different positions, (see the Fig.5.11).

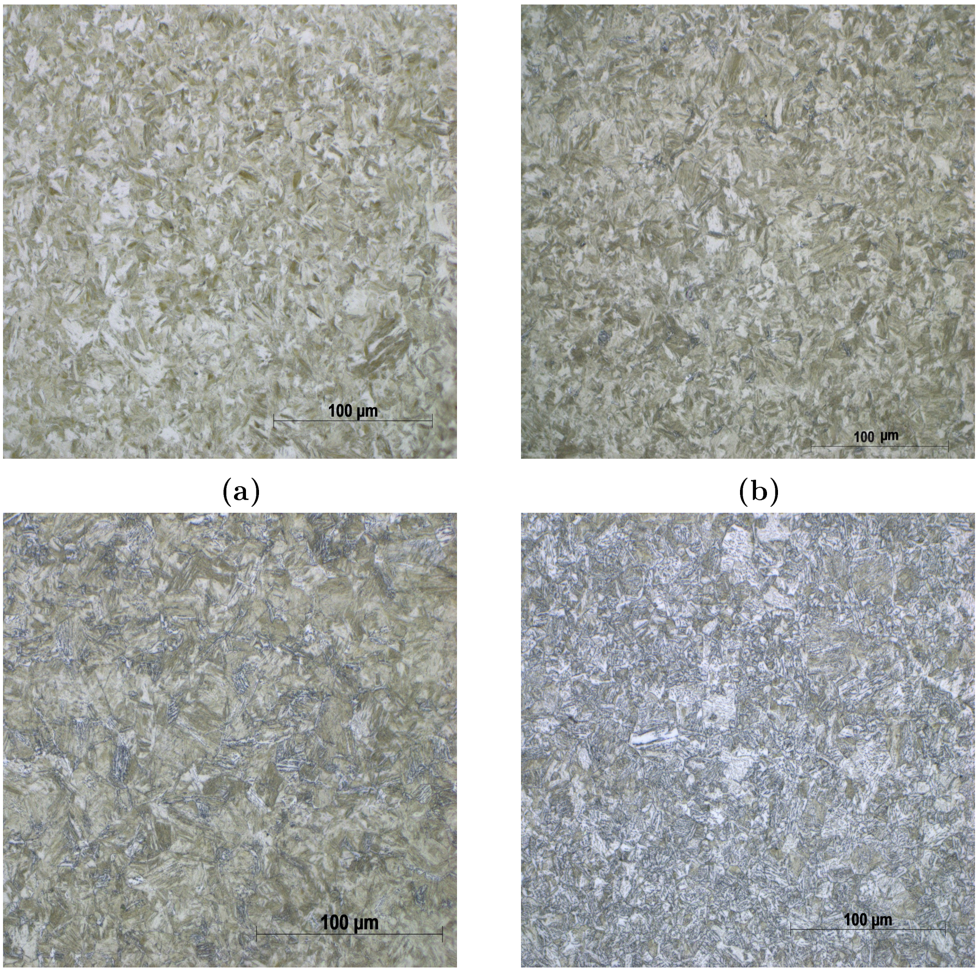

(a) (b) (c) (d)

Figure 5.11: Different micro-structures of Jominy sample with $T_P = 900°C$ as a function of distance **(a)** 0.3 mm from the quenched end **(b)** 3mm from the quenched end **(c)** 5mm from the quenched end **(d)** 11mm from the quenched end

The progress of phase transformations at a different distances from the quenched end as a result of cooling time,$\Delta t_{8/5}$, is showed on the Fig.5.11. At O.3 mm from the quenched end, upon very fast cooling, $\Delta t_{8/5} < 2.42s$, $\gamma \rightarrow \alpha$ transformation is assumed to be martenise, which corresponds to high hardness values above 450HV at that region. Furthermore, on the Fig.5.11**(b)**,**(c)** and **(d)**, upon slower cooling, $\Delta t_{8/5} = 2.42s, 8.23sand26s$, respectively, the changes through the micro-structure are quite obvious. At a distance 3mm from the quenched end, formation of upper bainite as a side needless/plates at the grain boundaries have started. This formation continued to grow as the distance from the quenched end increased and it is a reason why the hardness curve decreased gradually along the Jominy sample.

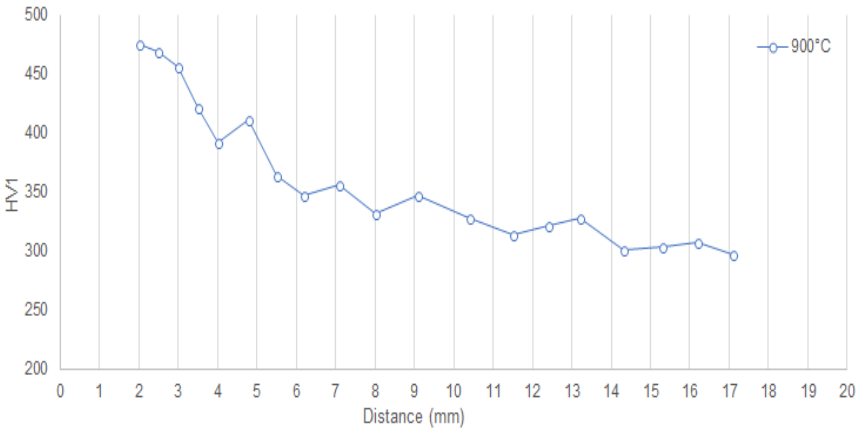

Figure 5.12: Measured hardness values for the Jominy sample with $T_P = 900°C$

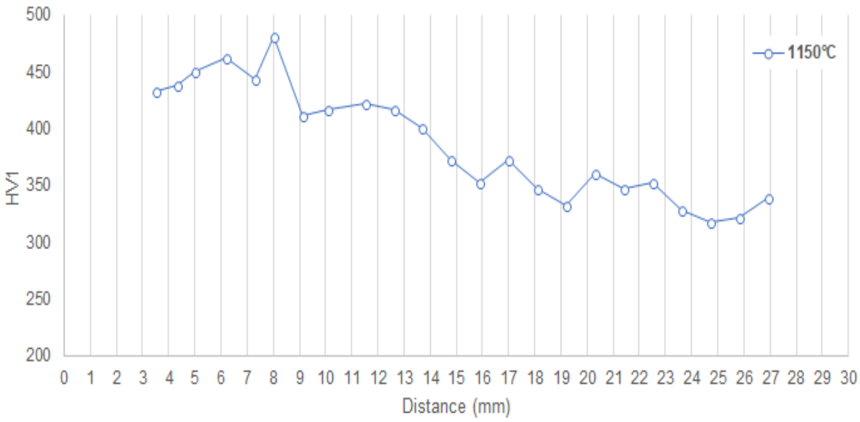

Figure 5.13: Measured hardness values for the Jominy sample with $T_P = 1150°C$

For the Jominy sample quenched from the higher temperature such as $1150°C$, the micro-structural changes as well as hardness values differed significantly when comparing to Jominy samples quenched from the lower temperatures (Fig.5.11. Micro-structural phase transformations corresponds to coarse grained zone, described in the Chapter 3. At very beginning (0.3 from the quenched end), very large austenite grains upon extremely high cooling transformed into brittle and hard martensite phases (Fig,5.14:**(a)**). The hardness values exceeded 400HV. When moving away from the quenched end,(at 3.2 mm), upon slower cooling, the small formation of upper bainite beggings to nucleate at the boundaries of the grains, (see Fig.5.14:**(c)**) and continues to spread along the Jominy sample, (see Fig.5.14). Furthermore, the loss in hardness over that range can be due to bainite distribution. Figure 5.14:**(f)**, shows the micro-structure that is formed at very slow cooling, (18mm away from the quenched end). The small formation of pearlite phases is observed, which can be related to small drop in the hardness since pearlitic structures are generally not strong and hard as bainitic phases, [7].

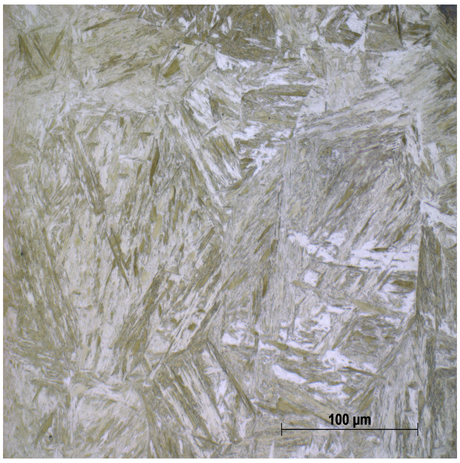

(a)

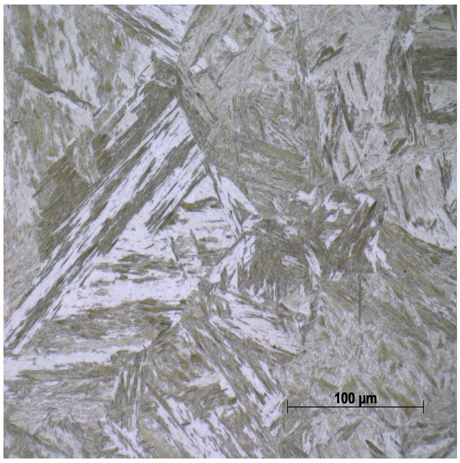

(b)

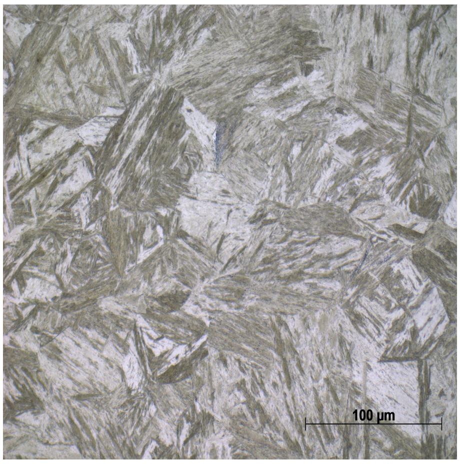

(c)

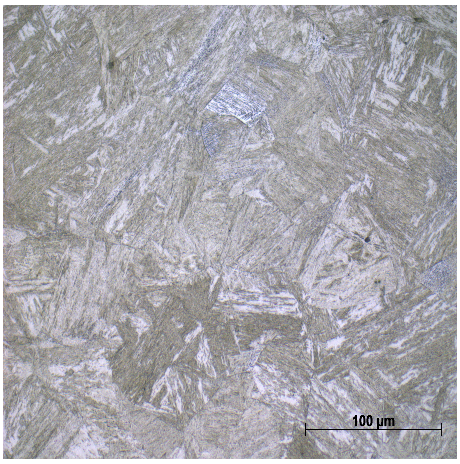

(d)

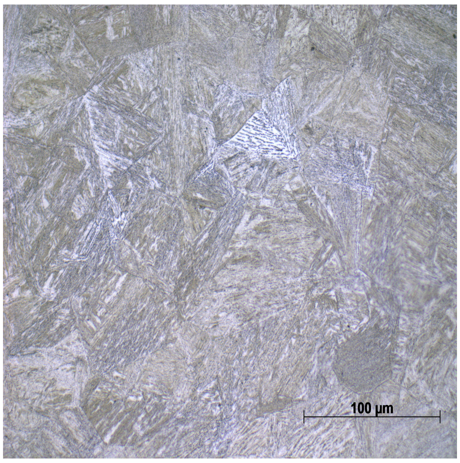

(e)

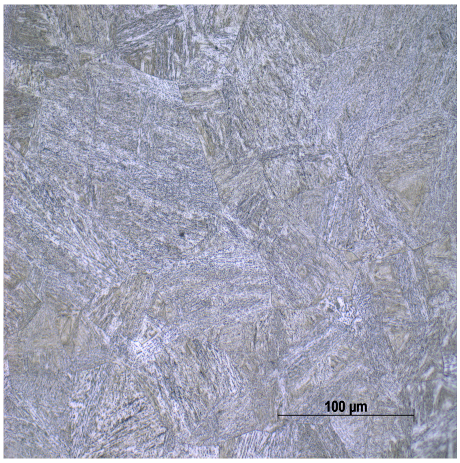

(f)

Figure 5.14: Different micro-structures of Jominy sample with $T_P = 1150°C$ as a function of distance **(a)** 0.3 mm from the quenched end **(b)** 0.7mm from the quenched end **(c)** 3mm from the quenched end **(d)** 8mm from the quenched end **(e)** 11mm from the quenched end **(f)** 18mm from the quenched end

5.2.3 The predicted and measured hardness curves

The results from Terasaki's predicted hardness method, was as already presented in the Chapter 4, Hardness prediction models. Those result are compared to the measured data from the Jominy sample with $T_P = 1150°C$ in the Fig.5.15. The maximum predicted hardness according to Terasaki method is 427HV while measured hardness for the Jominy sample at 3.5mm from the quenched end was 433HV. This shows that there is a relatively good agreement between the predicted hardness and the actual measured hardness on the Jominy sample as a function of cooling time. However, it seems that hardness values with increase in cooling time are higher in comparison to the predicted hardness values. Furtermore, higher hardness can be related to higher amount of martensite which also gives higher hardenability of the Jominy sample.

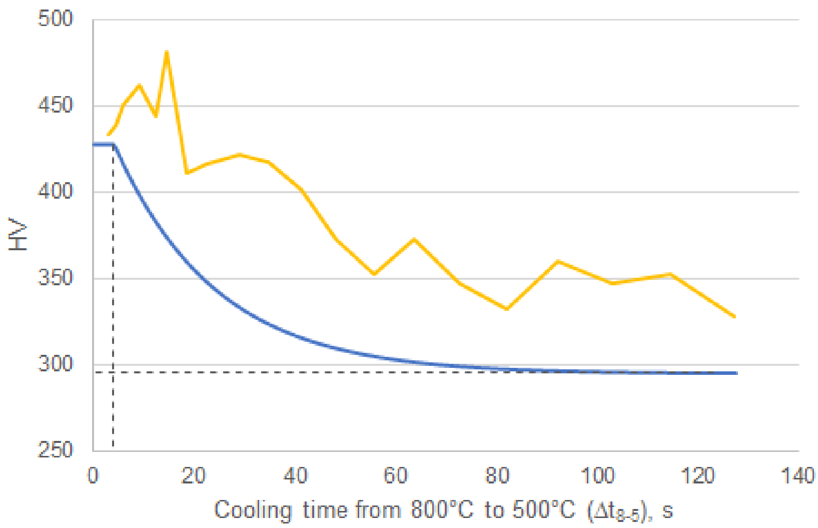

Figure 5.15: The comparison between predicted and measured maximum hardness as a function of cooling time

Chapter 6

Conclusion of the investigations

The effect of cooling time,$\Delta t_{8/5}$, on the micro-structural changes and hardness of the HAZ was investigated using three different approaches.
First, the Rosenthal equations were used in order to understand the temperature distribution over the HAZ as a function of peak temperature,T_P, heat input,Q, and preheat temperature,,T_0. The concept of cooling time through the range of 800-500 $\circ C$ was obtained from Rosenthal and later helped in analysing the micro-structural changes as function of cooling time,$\Delta t_{8/5}$. Results have showed that the cooling time increases with increasing the heat input and preheat temperatures. Therefore, higher cooling time, can help to avoid a formation of brittle martensite in the HAZ. Also the desired micro-structure can then be controlled by this variables and the desired hardness and toughness in the HAZ can be achieved. Therefore, the control of welding parameters such as heat input and cooling time, can help welder engineers to have a better overview over the changes in the micro-structure and mechanical properties of the final product during welding.

From the performed Jominy tests, the effects of three different austenitizing temperatures and cooling time on the hardness and micro-structural changes were investigated. The cooling time as a function of distance from the quenched end increases with increase of the distances. The results showed that increased in the cooling time decreased the hardness of the Jominy samples. Moreover, the amount of martensite decreased with the increase of cooling time. This resulted in formation of less brittle but stronger and ductile micro-structure at slower cooling time.

The maximum predicted hardness was employed by using the Terasaki hardness model. The predicted model compared to the actual hardness measurements from the Jominy sample. The predicted model showed a reasonable agreement with the measured hardness data from the Jominy. Knowing the composition of the steel, joint configuration and welding parameters, the welder engineer can estimate the maximum hardness of a HAZ by using a right prediction model. The method can therefore be used as a predictive tool in selecting appropriate welding procedures and it can help to reduce the number of welding qualification tests.

Bibliography

[1] Iso148 metallic materials - charpy pendulum impact test.

[2] Metallic materials - tensile testings - part 1:method of test at room temperature.

[3] M.F. Ashby and K.E. Easterling. A first report on diagrams for grain growth in welds. *Acta metall*, 1982.

[4] Kjeld Borggreen. Steels for high speed laser welding. *Force Institutes*, 1991.

[5] David Brandon and Wayne D. Kaplan. *Joining Proces; An Introduction*. Wiley, 1997.

[6] B. Buchmayr and J.S. Kirkaldy. Modeling of the temperature field, transformation behavior, hardness and mechanical respons of low alloy steels during cooling from the austenite region. *Springer-Verlag*, 1990.

[7] William D. Callister and David G. Rethwisch. *Material Science and Engineering*. Wiley, 2011.

[8] Kenneth E. Easterling David A. Porter and Mohamed Y. Sherif. *Phase Transformations in Metals and Alloys*. Taylor and Francis Group, 2009.

[9] Kenneth Easterling. *Introduction to the Psysical Metallurgy of Welding*. Butterworth & Co, 1983.

[10] Raymond A. Higgins. *Engineering Metallurgy*. Edward Arnold, 1993.

[11] D.G. Ivey K. Poorhaydari, B.M. Patchett. Estimation of cooling rate in the welding of plates with intermediate thickness. *Welding Journal*, 2005.

[12] J.C. Ion K.E Easterling and M.F. Asby. A second report on diagrams of microstructure and hardness for heat-affected zones in welds. *Acta metall*, 1984.

[13] Sindo Kou. *Welding Metallurgy*. Wiley.

[14] K.Suresh Kumar. Analytical modeling of temperature distribution, peak temperature, cooling rate and themal cycles in a solid work piece welded by laser welding process. *Procedia, Material Science*, 2014.

[15] Axel Lundberg. Temperature profiles and hardness estimation of laser welded heat affected zone in low carbon steel. Master's thesis, Faculty of Technology and scienec, Malmo University, Sweden, June,2014.

[16] A. Kermanpur M. E. Kahkhi and M. A. Golzar. Numerical simulation of contionus cooling of low alloy steel to predict microstructure and hardness. *IOP Publishing*, 2009.

[17] Z. Barsoum M. Khurshid and I. Barsoum. Load carrying capacities of butt welded joints in high strength steels. *Journal of Engineering Materials Technology*, 2015.

[18] Joanna M. Nicholas and David J. Abson. The prediction of maximum haz hardness in various regions of multiple pass welds. *The Welding Institute TWI*, June2008.

[19] M.I. Onsøien O.M Akselsen, G. Røkrvik and Ø. Grong. Assessment and predictions of haz tensile properties of high-strength steels. *Welding Research Council*, September,1989.

[20] D. A. Skobir R. Celin, J. Bernetic. Welding of steel grade s890ql. *Materials and Technology*, July,2014.

[21] R.E. Smallman and A.H.W. Ngan. *Modern Physical Metallurgy*. Elsevier, 2014.